Distributed Coordination of Flexible Loads Using Locational Marginal Prices

Distributed Coordination of Flexible Loads using Locational Marginal Prices

Xuan Gong, Antonio De Paola, *Member, IEEE,* David Angeli, *Fellow, IEEE,* and Goran Strbac, *Member, IEEE*

***Abstract*—This paper presents a novel distributed control strategy for large-scale deployment of flexible demand in power systems. A game theoretical setting is adopted, modelling the loads as rational players that aim to complete an assigned task at minimum cost and compete for power consumption at the cheapest hours of the day. The main novelty is the analysis of power systems with congestion: the proposed modelling framework envisages heterogeneous groups of loads that operate at different buses, connected by transmission lines of limited capacity. The locational marginal prices of electricity, different in general for each bus, are calculated through an optimal power flow problem, accounting for the impact of the flexible devices on power demand and generation. A new iterative scheme for flexible demand coordination is analytically characterized as a multi-valued mapping. Its convergence to a stable market configuration (i.e. variational Wardrop equilibrium) and global optimality are analytically demonstrated, for any penetration level of flexible demand and any grid topology. Distributed implementations of the proposed control strategy are discussed, evaluating their performance with simulations on the IEEE 24-bus system.**

***Index Terms*—Flexible demand, distributed control, transmission network, locational marginal prices, game theory.**

I. Introduction

A. Motivation

The penetration of flexible loads, such as smart appliances and electric vehicles, is expected to increase significantly in the future, with significant potential benefits. The electrification of transportation can mitigate the shortage of fossil fuels and improve energy efficiency [1], while the increasing flexibility of demand can be exploited to provide ancillary services [2]. On the other hand, the growing penetration of flexible loads has certain potential drawbacks [3], [4]. For instance, the diffusion of flexible loads will change consumption patterns, potentially causing new demand peaks and significant voltage deviations in the power grid. Proper coordination of flexible appliances can avoid such undesirable effects and, at the same time, facilitate the integration of renewables, reduce operating cost and improve stability and reliability of the grid [5], [6].

B. Relevant work

A consistent amount of research has been carried out to achieve flexible demand coordination, evaluating centralized and decentralized approaches. Centralized control strategies such as [7], [8] envision a central entity that collects information from all flexible appliances and centrally determines their power consumption in order to optimize some global objectives. However, these schemes become complicated to implement and computationally expensive for large numbers of flexible appliances, making them unsuitable for big and complex systems. Better scalability is obtained with distributed schemes that also preserve the privacy of the appliances. Multiple decentralized approaches have been considered, including Lagrange relaxation methods [9], congestion pricing [10] and stochastic pricing [11]. Game theory has also been extensively applied to devise distributed control strategies for coordination of flexible loads [12]–[18]. The general approach adopted in these papers is to model the flexible loads as self-interested players that compete for energy consumption at the cheapest prices. On this basis, distributed control actions are designed in order to converge to a stable market outcome (characterized as a Nash equilibrium) and to possibly maximize social welfare.

It is worth noting that all these works consider a unique price function throughout the grid, repartitioning total costs among the users proportionally to their fraction of total power consumption [12] or assuming that the electricity price is some monotone increasing function of total power demand [13]–[18]. This choice captures a fundamental property of electricity markets, where the marginal cost of generation is increasing and higher supply corresponds to higher prices. However, the proposed modelling frameworks only consider distribution networks [13], [17], [18] or conduct a whole-system analysis [14]–[16] that does not account for any underlying network topology. Moreover, the pricing schemes in [12]–[18] neglect two fundamental characteristics of realistic power grids: the presence of multiple buses (connected by transmission lines of limited capacity) and, as a result, the arising of different locational marginal prices (LMPs) throughout the system.

Recent work has proposed novel modelling approaches that incorporate the transmission network, investigating the impact of EVs [19], [20], and more generally demand response [21], [22] on LMPs. The interactions between distribution and transmission and the impact of uncertainties have also been assessed in [23] and [24], respectively. However, differently from [12]–[18], all the cited papers [19]–[24] do not provide any theoretical guarantee on the convergence to equilibrium and social optimality of their coordination scheme.

C. Contributions

The objective of this paper is to bridge the gap between the research approaches presented in [12]–[18] and in [19]–[24].

X. Gong, (corresponding author - e-mail: xuan.gong15@imperial.ac.uk), D. Angeli and G. Strbac are with the Dept. of Electrical & Electronic Engineering, Imperial College, London. A. De Paola is with the Dept. of Electronic & Electrical Engineering of the University of Bath. D. Angeli is also with the Dept. of Information Engineering of the University of Florence.
This work was supported by the Leverhulme Trust, Grant ECF-2016-394. X. Gong and A. De Paola contributed equally to this work.

In particular, the framework presented in this work combines a rigorous theoretical analysis (guaranteeing convergence and optimality of the proposed coordination scheme) with an explicit modelling of the transmission infrastructure (accounting for the underlying network topology and assessing the impact of demand response on LMPs and generation costs).

These results are obtained considering heterogeneous price-responsive loads operating at distinct buses of the power system. The congestion of transmission lines is taken into account and the LMPs at each bus are characterized as the Lagrange multipliers associated to a linearized AC optimal power flow (ACOPF) problem, whose solution depends on the operation strategy of the flexible loads. The proposed coordination scheme for flexible demand relies on the preliminary findings of [25] and envisions iterative better-response updates by the price-responsive appliances, which are characterized as the evolution of a multi-valued mapping. The formulation and the results of [25] have been expanded to explicitly consider a more complex pricing structure with LMPs. In order to account for the congestion of the transmission lines and the potential price jumps that this might cause, a more general class of aggregative games has been considered and a novel notion of variational Wardrop equilibrium is introduced. Through the application of Lyapunov tools, it is demonstrated that the proposed coordination scheme converges to an equilibrium and achieves global optimality for any penetration level of flexible demand and any grid topology. Distributed implementations of the proposed scheme and simulative results on the IEEE 24-bus system are also provided.

D. Paper structure

The rest of the paper is structured as follows. Section II describes the chosen power system model and the properties of the linearized ACOPF solution. Section III presents the modeling of the flexible appliances and the considered game-theoretical setup. Section IV proposes a distributed scheme for flexible demand coordination and demonstrates its convergence and optimality properties. The performance of the proposed control strategy, including its robustness with respect to uncertainties, is evaluated in simulation in Section V, while Section VI contains some concluding remarks.

II. Modelling of Optimal Power Flow and Electricity Prices

The considered power system is composed by a finite set $\mathscr{M} = \{1,\dots,M\}$ of distinct buses. The set of transmission lines (of limited capacity) linking two buses is denoted as $\mathscr{L} = \{1,\dots,L\}$, with $s(l)$, $r(l) \in \mathscr{M}$ indicating the reference sending and receiving nodes of line l, respectively. A linearized ACOPF problem is solved over the discrete time interval $\mathscr{T} = \{1,\dots,T\}$. We denote by $D \in \mathbb{R}^{MT}$ and $DQ \in \mathbb{R}^{MT}$ the vectors of active and reactive power demand. The single components $D_{m,t}$ and $DQ_{m,t}$ correspond to the total active and reactive power demand at bus m at time t. A similar vector notation is adopted for active and reactive generation (G and GQ, respectively), voltage angles θ and voltage magnitudes v, denoting by $G_{m,t}$, $GQ_{m,t}$, $\theta_{m,t}$ and $v_{m,t}$ their scalar values for bus m and time t. The formulation in [26] is adopted for the linearized ACOPF:

$$\varphi(D) = \min_{G,GQ,\theta,v^2} \sum_{m=1}^{M}\sum_{t=1}^{T} f_m(G_{m,t}) \tag{1}$$

subject to $(\forall l \in \mathscr{L}, m \in \mathscr{M}, t \in \mathscr{T})$:

$$P_{l,t} = g_l \frac{v^2_{s(l),t} - v^2_{r(l),t}}{2} - b_l\left[\theta_{s(l),t} - \theta_{r(l),t}\right] + P^L_{l,t} \tag{2a}$$

$$Q_{l,t} = -b_l \frac{v^2_{s(l),t} - v^2_{r(l),t}}{2} - g_l\left[\theta_{s(l),t} - \theta_{r(l),t}\right] + Q^L_{l,t} \tag{2b}$$

$$G_{m,t} - D_{m,t} = \sum_{\{l:s(l)=m\}} P_{l,t} - \sum_{\{l:r(l)=m\}} P_{l,t} + \sum_{n=1}^{M} \mathscr{G}_{mn} v^2_m \tag{2c}$$

$$GQ_{m,t} - DQ_{m,t} = \sum_{\{l:s(l)=m\}} Q_{l,t} - \sum_{\{l:r(l)=m\}} Q_{l,t} - \sum_{n=1}^{M} \mathscr{B}_{mn} v^2_m \tag{2d}$$

$$\underline{G}_m \le G_{m,t} \le \bar{G}_m \tag{2e}$$

$$\underline{GQ}_m \le GQ_{m,t} \le \bar{GQ}_m \tag{2f}$$

$$\underline{v}^2_m \le v^2_{m,t} \le \bar{v}^2_m \tag{2g}$$

$$\underline{\theta}_m \le \theta_{m,t} \le \bar{\theta}_m \tag{2h}$$

$$\Big(\sin(2\pi c/a) - \sin(2\pi(c-1)/a)\Big)\cdot P_{l,t} - \sin(2\pi/a)\cdot \bar{S}_l$$
$$-\Big(\cos(2\pi c/a) - \cos(2\pi(c-1)/a)\Big)\cdot Q_{l,t} \le 0 \quad c = 1,\dots,a \tag{2i}$$

The linearized ACOPF in (1)-(2) determines active (and reactive) power generation G (and GQ), voltage angles θ and squared voltage magnitude v^2 that minimize generation costs. The function $f_m(g)$ in (1) is the cost of generating g units of power at bus m and is assumed to be strictly convex. Constraints (2a)-(2b) are the linearized expressions of active (and reactive) power flow $P_{l,t}$ (and $Q_{l,t}$) on line l, where g_l and b_l are conductance and susceptance of the line. Details on the expressions and linearization of the power losses terms $P^L_{l,t}$ and $Q^L_{l,t}$ are in [26]. Constraints (2c)-(2d) are the nodal balance expressions for active and reactive power. The last sums in their right-hand side represent the power flows on the shunt elements, where $\mathscr{G}$ and $\mathscr{B}$ are the real and imaginary part of the admittance matrix. Bounds on G, GQ, v^2 and θ are imposed in (2e)-(2h). The capacity constraint $P^2_{l,t} + Q^2_{l,t} \le \bar{S}^2_l$ of line l at time t is represented in (2i) by a piecewise linearization [27] which approximates the circle $P^2_{l,t} + Q^2_{l,t} = \bar{S}^2_l$ in the P-Q plane as a convex regular polygon of a sides.

A. Electricity prices

In order to characterize the locational marginal prices associated to a certain vector of demand values D, some properties of $\varphi(D)$ are preliminarily discussed.

Proposition 1: The minimized generation cost $\varphi(D)$ is a strictly convex function on any set $[D_{\min}, D_{\max}]^{MT} \subset \mathbb{R}^{MT}_{+}$.

Proof: See Appendix A. ■

From the convexity result of Proposition 1, $\varphi(D)$ is Lipschitz continuous on some open interval $(D_{min}, D_{max})^{MT}$ including all feasible values of demand. It straightly follows

that $\varphi(D)$ is differentiable almost everywhere [28], with the exception of some zero-measure set $\mathscr{D} \subset (D_{min}, D_{max})^{MT}$. Introducing the notion of sub-differential, we can write:

$$\frac{\partial \varphi(D)}{\partial D_{m,t}} = \begin{cases} \varphi'_{m,t}(D) & \text{if} \quad D \notin \mathscr{D} \\ \left[\underline{\varphi}'_{m,t}(D), \bar{\varphi}'_{m,t}(D)\right] & \text{if} \quad D \in \mathscr{D} \end{cases} \tag{3}$$

where $\underline{\varphi}'_{m,t}(D)$ and $\bar{\varphi}'_{m,t}(D)$ are the left and right partial derivatives of $\varphi(D)$ with respect to $D_{m,t}$.

The electricity price $p_{m,t}$ is chosen as the Lagrange multiplier associated to the power balance constraint (2c), i.e. the marginal cost of providing an additional unit of power at bus m at time t. Within the considered theoretical framework, this price corresponds to the partial derivative presented in (3). To account for the points of non-differentiability of the optimized cost $\varphi(D)$, two distinct price signals are considered:

$$\underline{p}_{m,t}(D) = \begin{cases} \varphi'_{m,t}(D) & \text{if} \quad D \notin \mathscr{D} \\ \underline{\varphi}'_{m,t}(D) & \text{if} \quad D \in \mathscr{D}. \end{cases} \tag{4a}$$

$$\bar{p}_{m,t}(D) = \begin{cases} \varphi'_{m,t}(D) & \text{if} \quad D \notin \mathscr{D} \\ \bar{\varphi}'_{m,t}(D) & \text{if} \quad D \in \mathscr{D}. \end{cases} \tag{4b}$$

Under the current formulation, $\bar{p}_{m,t}$ is the marginal cost of providing an additional unit of power at bus m. Conversely, $\underline{p}_{m,t}$ represents the marginal saving of reducing by one unit the power supplied to bus m.

We wish to emphasize that the double price formulation in (4) is not only a mathematical technical detail but it also represents a crucial element in correctly characterizing price variations and the cost minimization of the loads. In particular, the proposed formulation allows to formally account for the price "jumps" resulting from a marginal generator reaching its maximum capacity or the saturation of some line. In these cases, the electricity price will vary discontinuously. Considering the corresponding value of the demand vector D, the quantities $\underline{p}_{m,t}(D)$ and $\bar{p}_{m,t}(D)$ will represent the different price values at bus m and time t before and after the jump. It follows that $D \in \mathscr{D}$ and the minimized cost function $\varphi(D)$ will not be differentiable in these particular cases.

The price discontinuities are particularly relevant in the cost minimization problem of flexible demand. Each load, in order to correctly evaluate its cost variation, will have to consider $\underline{p}_{m,t}$ when its power consumption is reduced (thus reducing total demand D) and $\bar{p}_{m,t}$ when its power consumption is increased (thus increasing total demand D). This is consistent with the equilibrium formulation in Definition 2, where the considered prices are selected accordingly to the sign of the associated power scheduling variation.

B. Local monotonicity of prices

As a preliminary step in the definition of the proposed control scheme and in the theoretical assessment of its convergence and optimality properties, an important monotonicity property of the prices in (4) is presented.

Proposition 2: Assume strict convexity of the generation cost functions $f_m(G)$ in (1). For any bus $m \in \mathscr{M}$ and time $t \in \mathscr{T}$, the corresponding electricity prices $\bar{p}_{m,t}(D)$ and $\underline{p}_{m,t}(D)$ are monotone increasing with respect to demand $D_{m,t}$ at the same bus m and time instant t.

Proof: See Appendix B. ■

From the above considerations, the following power quantity can now be introduced:

Definition 1: Consider a demand vector $D \in \mathbb{R}^{MT}$, a bus $m \in \mathscr{M}$ and two time instants $\bar{t}, \underline{t} \in \mathscr{T}$. The quantity $\varepsilon(D, m, \bar{t}, \underline{t})$ is defined as follows:

$$\begin{aligned} \varepsilon(D, m, \bar{t}, \underline{t}) := \arg\min_{x \geq 0} \big(\big| & \bar{p}_{m,\bar{t}}(D + x \cdot (\hat{\mathbf{e}}_{m,\bar{t}} - \hat{\mathbf{e}}_{m,\underline{t}})) \\ & - \underline{p}_{m,\underline{t}}(D + x \cdot (\hat{\mathbf{e}}_{m,\bar{t}} - \hat{\mathbf{e}}_{m,\underline{t}})) \big| \big) \end{aligned} \tag{5}$$

where $\hat{\mathbf{e}}_{m,t}$ is the unit vector of the standard orthogonal basis associated to bus m and time t.

In the above definition, ε is the positive amount of power that can be swapped between $\underline{t}$ ant $\bar{t}$ in order to minimize their price differential. From the monotonicity of $\underline{p}_{m,t}$ and $\bar{p}_{m,t}$, when $\bar{p}_{m,\bar{t}} \leq \underline{p}_{m,\underline{t}}$ the quantity ε corresponds to the maximum power swap between $\underline{t}$ and $\bar{t}$ that preserves their original price order.

Remark 1: The price monotonicity introduced in Proposition 2 is used to formally prove convergence to equilibrium of the proposed control scheme. This convergence result can still be proven in more general contexts where the considered OPF problem is not convex and the price monotonicity is not guaranteed. In this case, it is sufficient to verify (21a) through a Taylor expansion of the minimized cost φ and replace ε in (5) by a suitable "sufficiently small" power variation.

III. Modelling of flexible demand

This section presents the modelling framework of the flexible loads. These are described as price-responsive rational agents, characterizing their interactions through a game-theoretical set-up and introducing the concept of variational Wardrop equilibrium.

A. Individual devices and impact on aggregate power demand

A population $\mathscr{N} = \{1, \ldots, N\}$ of price-responsive devices is considered, denoting by $\mu_j \in \mathscr{M}$ the power system bus in which the flexible load $j \in \mathscr{N}$ operates. The flexible appliances are considered as self-interested rational agents that operate over the discrete time interval $\mathscr{T} = \{1, \ldots, T\}$. In particular, each appliance $j \in \mathscr{N}$ schedules its power consumption over time $u_j = \left[u_{j,1}, \ldots, u_{j,T}\right] \in \mathbb{R}^T$ in order to complete an assigned task at minimum energy cost. The task of agent j can be unequivocally characterized by three quantities:

- Its rated power P_j.
- The total energy E_j required to complete its task.
- The set of time instants $\mathscr{A}_j \subseteq \mathscr{T}$ during which it is available to operate.

Any feasible power consumption profile u_j guaranteeing task completion for agent j belongs to the set $\mathscr{U}_j$, defined as:

$$\begin{aligned} \mathscr{U}_j := \Bigg\{ u_j \in \mathbb{R}^T : \; & \sum_{t=1}^{T} u_{j,t} \cdot \Delta t = E_j \,, \\ & 0 \leq u_{j,t} \leq P_j \cdot \mathbb{1}_{\mathscr{A}_j}(t) \quad \forall t \in \mathscr{T} \Bigg\} \end{aligned} \tag{6}$$

where Δt denotes the time discretization step and $\mathbb{1}_{\mathscr{S}}(t)$ is the indicator function:

$$\mathbb{1}_{\mathscr{S}}(t) = \begin{cases} 1 & \text{if} \quad t \in \mathscr{S} \\ 0 & \text{if} \quad t \notin \mathscr{S}. \end{cases} \tag{7}$$

The equality in (6) ensures that the total energy consumed by appliance j is equal to the energy required to complete its task. The inequalities in (6) impose that the (positive) power consumption of appliance j cannot exceed its rated power P_j for t within the availability interval $\mathscr{A}_j$ and must be zero for t outside it. The proposed notation can be extended, representing by $u = [u_1, \dots, u_N] \in \mathbb{R}^{NT}$ the scheduled power profile of the whole population and by $\mathscr{U} = \mathscr{U}_1 \times \cdots \times \mathscr{U}_N$ the corresponding feasibility set.

Assumption 1: The power scheduling problem admits at least one solution. In other words, the parameters $(P_j, E_j, \mathscr{A}_j)$ of each device j are such that $\mathscr{U} \neq \varnothing$.

In order to account for the impact of the flexible appliances on the power system quantities discussed in Section II, it is sufficient to replace the demand vector $D \in \mathbb{R}^{MT}$ with a function $D(u) : \mathscr{U} \to \mathbb{R}^{MT}$ of the power scheduling u. For the individual demand component $D_{m,t}$, it holds:

$$D_{m,t}(u) = d_{m,t} + \sum_{\{j:\mu_j=m\}} u_{j,t} \tag{8}$$

where $d_{m,t}$ is the known inflexible demand at bus m at time t.

Remark 2: Consistently with previous works [19]–[22], [24] on the subject, the proposed modelling framework directly considers the impact of flexible demand at a transmission level and it does not specifically account for the effects on the underlying distribution network. As discussed in Section VI, an explicit characterization of the distribution network will be a key direction for further research in this area.

B. Game-theoretical framework and Wardrop equilibrium

The coordination of the power scheduling by the flexible appliances is analyzed within a game-theoretical framework. Each device is modeled as a self-interested player that aims to minimize its individual cost in response to broadcast price signals. The following competitive game is considered:

- *Players:* The set $\mathscr{N}$ of flexible devices.
- *Strategies:* The set $\mathscr{U}_j$ of feasible power profiles for a single flexible device $j \in \mathscr{N}$.
- *Objective function:* Energy cost of task completion. For a certain price signal $p : \mathscr{T} \to \mathbb{R}_+$, the following expression can be provided for the cost C_j of device j:

$$C_j = \sum_{t=1}^{T} p_t \cdot u_{j,t} \Delta t. \tag{9}$$

Within this framework, the flexible loads are rational agents competing for power consumption at cheap prices. In the next section, we propose a coordination strategy of the devices that ensures convergence to a stable market configuration. This is expressed as a variational Wardrop equilibrium, defined next.

Definition 2: The scheduled power consumption $u^* \in \mathscr{U} \subset \mathbb{R}^{NT}$ corresponds to a variational Wardrop equilibrium if the following holds for all $u \in \mathscr{U}$:

$$\begin{aligned} \Delta C_j = &\sum_{t:\, u_{j,t} \geq u^*_{j,t}} \bar{p}^*_{\mu_j,t} \left[u_{j,t} - u^*_{j,t}\right] \Delta t \\ &- \sum_{t:u_{j,t} \leq u^*_{j,t}} \underline{p}^*_{\mu_j,t} \left[u^*_{j,t} - u_{j,t}\right] \Delta t \geq 0 \end{aligned} \qquad \forall j \in \mathscr{N} \tag{10}$$

$$\underline{p}^*_{m,t} = \underline{p}_{m,t}\left(D(u^*)\right) \quad \bar{p}^*_{m,t} = \bar{p}_{m,t}\left(D(u^*)\right) \quad \forall m \in \mathscr{M}, \forall t \in \mathscr{T}. \tag{11}$$

This definition represents an extension of the Wardrop equilibrium concept (or aggregative equilibrium), which has already been applied in the context of price-responsive demand coordination [14], [29], [30]. The general idea in these works is to characterize the equilibrium as a fixed point: the power scheduling of each device is optimal for a certain price signal and, at the same time, the aggregate power consumption of all loads induces that very same price. This concept satisfyingly approximates a Nash equilibrium if the effect of the individual player on the global quantities of the system is negligible. This is true in the present case of large-scale deployment of flexible demand, as the power consumption of a single device is orders of magnitude smaller than total power demand.

Definition 2 proposes a generalization of the Wardrop equilibrium concept for the case of non-differentiable global cost functions and discontinuous LMPs which, as underlined in our analysis, naturally arise from line congestion and maximum generation capacity when the proposed linearized ACOPF is considered. The left-hand side of (10) denotes the energy cost variation ΔC_j incurred by the single device j if it switches from the candidate equilibrium solution u^*_j to some other feasible power profile $u_j \in \mathscr{U}_j$. This cost variation is the difference between the costs of increased power consumption at certain time instants (priced at $\bar{p}^*$) and the savings from reduced power consumptions at other times (priced at $\underline{p}^*$). At equilibrium, as imposed in (10), the cost variations ΔC_j associated to a different strategy are always greater or equal than zero. Note that, if the minimized generation cost $\varphi(D)$ is a function differentiable everywhere, the signals $\bar{p}^*$ and $\underline{p}^*$ are the same, leading to the classical definition of Wardrop equilibrium. The second part of the fixed point condition is given by (11), which ensures that the overall power consumption of the devices leads to same prices $\bar{p}*$ and $\underline{p}^*$ considered in (10).

In order to derive an equilibrium condition that is equivalent to the definition in (10), to be used in the subsequent analysis, the following function is introduced:

$$\gamma(u, j, \bar{t}, \underline{t}) := \left(\underline{p}_{\mu_j \underline{t}}(D(u)) - \bar{p}_{\mu_j \bar{t}}(D(u))\right)\left(P_j - u_{j\bar{t}}\right) u_{j\underline{t}}. \tag{12}$$

The sign of γ indicates the possibility by the single load to reduce its cost. If $\gamma(u, j, \bar{t}, \underline{t}) > 0$, the device j operating at bus μ_j, starting from a schedule u, can reduce its cost by swapping power from time $t = \underline{t}$ to time $t = \bar{t}$. In fact, considering the non-negativity of the factors $(P_j - u_{j\bar{t}})$ and $u_{j\underline{t}}$ in (12), the condition $\gamma(u, j, \bar{t}, \underline{t}) > 0$ implies three distinct inequalities:

$$\underline{p}_{\mu_j \underline{t}}(D(u)) > \bar{p}_{\mu_j \bar{t}}(D(u)) \qquad u_{j\bar{t}} < P_j \qquad u_{j\underline{t}} > 0.$$

The conditions above indicate, respectively, that:

- An advantageous price difference exists between $\underline{t}$ and $\bar{t}$.
- The device j can consume more power at time $\bar{t}$.
- The device j can consume less power at time $\underline{t}$.

The last two points make the power swap between $\underline{t}$ and $\underline{t}$ feasible, while the first one makes it cost-reducing for the device j. It follows that an equilibrium is reached when γ is always non positive and no device can perform a cost-reducing power swap. This is formalized by the following result:

Proposition 3: The scheduled power consumption $u^* \in \mathscr{U}$ corresponds to a variational Wardrop equilibrium, as presented in Definition 2, if and only if:

$$\gamma(u^*, j, \bar{t}, \underline{t}) \leq 0 \quad \forall j \in \mathscr{N}, \quad \forall (\bar{t}, \underline{t}) \in \mathscr{A}_j \times \mathscr{A}_j. \tag{13}$$

Proof: See Appendix C ∎

IV. Distributed Coordination of Flexible Demand

This section proposes a distributed control strategy for flexible demand coordination. This is initially characterized in Section IV-A as a multi-valued mapping, theoretically demonstrating with Lyapunov techniques and convexity arguments its asymptotic convergence to a variational Wardrop equilibrium that is also socially optimal. An equivalent pseudo-code algorithm representation is given in Section IV-B, whereas Section IV-C discusses the implementation of the proposed control strategy in practical contexts, envisioning a distributed scheme where individual appliances iteratively update their power scheduling, on the basis of broadcast price signals, in order to reduce their energy cost.

A. Power update as evolution of dynamical system

The power scheduling update of the flexible appliances is described by the following discrete-time dynamical system:

$$u(0) = u^0 \in \mathscr{U} \qquad u(k+1) \in F(u(k)) \tag{14}$$

where $F : \mathscr{U} \mapsto \mathscr{U}$ is a multi-valued correspondence and $u(k)$ denotes the scheduled power consumption of the flexible loads after k iterations of the proposed coordination strategy.

In order to characterize the multi-valued mapping F, the following quantities are preliminarily introduced:

$$S_j(u) := \underset{(\bar{t}, \underline{t}) \in \mathscr{A}_j \times \mathscr{A}_j}{\arg\max} \ \gamma(u, j, \bar{t}, \underline{t}) \tag{15}$$

$$\Delta(u, j, \bar{t}, \underline{t}) := \min\left(\left\{\varepsilon(D(u), \mu_j, \bar{t}, \underline{t}), P_j - u_{j,\bar{t}}, u_{j,\underline{t}}\right\}\right) \tag{16}$$

The set $S_j(u)$ associates to a device $j \in \mathscr{N}$ the pairs of time instants $s_j = (\bar{t}_j, \underline{t}_j)$ that maximize the function γ under the current u and can therefore be considered for cost-reducing power swaps. Considering the constraints in (6) and Definition 1 for ε, the function Δ returns the maximum feasible power swap that device j can perform between $\bar{t}$ and $\underline{t}$ while preserving their original price order.

The multi-value mapping F_j associated to the power scheduling update of a single device j is now defined:

$$F_j(u) = \bigcup_{s_j \in S_j(u)} f^{(s_j)}(u) = \bigcup_{s_j \in S_j(u)} \left[f_{1,1}^{(s_j)}(u), \ldots, f_{N,T}^{(s_j)}(u) \right] \tag{17}$$

where the single component $f_{i,t}^{(s_j)}(u)$ of $f^{(s_j)}(u)$ in (17), corresponding to the updated power consumption of device i at time t, has the following expression when $s_j = (\bar{t}, \underline{t})$:

$$f_{i,t}^{(s_j)}(u) = u_{i,t} + \Delta(u, j, \bar{t}, \underline{t}) \cdot \mathbb{1}_{\{j\}}(i) \left[\mathbb{1}_{\{\bar{t}\}}(t) - \mathbb{1}_{\{\underline{t}\}}(t) \right]. \tag{18}$$

When the mapping $F_j(u)$ in (17) is applied, a single element $s_j = (\bar{t}_j, \underline{t}_j)$ is selected within the set $S_j(u)$ and the device j swaps power from time $\underline{t}_j$ to $\bar{t}_j$. The amount of swapped power corresponds to Δ, defined in (16). The last two terms in its minimum function ensure that the updated power scheduling remains feasible, whereas the first term ε, defined in (5), guarantees that the power swap is performed (i.e. $\Delta > 0$) only if there is an advantageous price differential between the time instants $\bar{t}_j$ and $\underline{t}_j$. All other devices $i \in \mathscr{N} \backslash \{j\}$ maintain their previous power scheduling. The complete multi-valued correspondence F in (14) can now be expressed as the composition of N mappings F_j, iterated over the whole population of flexible appliances $\mathscr{N} = \{1, \ldots, N\}$:

$$F(u) := (F_N \circ \cdots \circ F_1)(u). \tag{19}$$

The evolution of the power scheduling $u(k)$ according to the proposed update strategy can now be characterized as follows:

Definition 3: Given the dynamical system (14), with F defined in (19), its solution set Ψ can be expressed as:

$$\Psi := \left\{ \psi : \mathbb{N} \to \mathscr{U} \ : \ \psi(k+1) \in F(\psi(k)) \ \ \forall k \in \mathbb{N} \right\}. \tag{20}$$

Some fundamental properties of the solution set Ψ are now demonstrated, showing that the proposed power update strategy (characterized by the mapping F) always converges to the variational Wardrop equilibrium presented in Definition 2.

This is proved with Lyapunov arguments, selecting the optimized generation costs $\varphi(D)$ as the considered Lyapunov function. Similarly to the Lyapunov stability theorem in the discrete-time case, we aim to demonstrate that the function $\varphi(D)$ is always nonincreasing when evaluated over the state trajectories (19) of system (14), as shown in Proposition 4. This implies convergence to equilibrium – as demonstrated in Theorem 1.

The first step in our analysis is the following result:

Proposition 4: For the optimized generation cost φ presented in (1), evaluated along any solution $\psi \in \Psi$, it holds:

$$\varphi(D(\psi(k+1))) \leq \varphi(D(\psi(k))) \qquad \forall k \in \mathbb{N} \tag{21a}$$

$$\psi(k+1) = \psi(k) \qquad \forall k : \varphi(D(\psi(k+1))) = \varphi(D(\psi(k))) \tag{21b}$$

$$\lim_{k \to \infty} \varphi(D(\psi(k))) = \varphi_\infty, \quad \varphi_\infty \in \mathbb{R}_+ \tag{21c}$$

Proof: See Appendix D. ∎

Proposition 4 shows that the proposed power update of the flexible appliances, characterized by the multivalued mapping F, has the fundamental property of reducing the total generation costs of the system at each iteration. As a result, the minimized generation cost φ asymptotically converges to some finite value φ_∞. In addition, from (21b), the proposed strategy updates the power scheduling of the appliances only if this ensures a reduction of total costs. The main equilibrium and optimality results can now be provided.

Theorem 1: Let Ω^* denote the set of variational Wardrop equilibria introduced in Definition 2. Indicating by $|x|_\Gamma$ the distance between some element $x \in \mathscr{U}$ and the set $\Gamma \subseteq \mathscr{U}$, it holds:

$$\lim_{k \to \infty} |\psi(k)|_{\Omega^*} = 0 \qquad \forall \psi \in \Psi. \tag{22}$$

Proof: See Appendix E. ∎

This result ensures that the proposed scheme asymptotically converges to the set of variational Wardrop equilibria. In

other words, when the final power scheduling is applied, each device has no unilateral interest in modifying its power consumption in order to reduce its energy cost. This property holds for any grid topology, any penetration level of flexible demand and all parameters of the price-responsive appliances. Global optimality of the Wardrop equilibrium can also be demonstrated, under some mild assumptions:

Theorem 2: If the optimized generation cost is differentiable at the Wardrop equilibrium $u^* \in \Omega^*$, i.e. $D = D(u^*) \notin \mathscr{D}$ in (3), the following optimality property is verified:

$$\varphi(D(u^*)) \leq \varphi(D(u)) \qquad \forall u \in \mathscr{U}. \tag{23}$$

Proof: See Appendix F. ■

The theorem shows that any Wardrop equilibrium u^* is also socially optimal if the function $\varphi(D)$ is differentiable at $D = D(u^*)$. In these cases, there exists no feasible power scheduling $u \in \mathscr{U}$ whose associated generation cost $\varphi(D(u))$ is lower than $\varphi(D(u^*))$ obtained at equilibrium.

B. Pseudo-Code and Flowchart Representation

Algorithm 1 Iterative scheme - Flex. demand coordination

1) **Initialization phase.** Starting values for power scheduling of the appliances and flag variables are set:
$$u(0) = u^0 \in \mathscr{U} \qquad k = 0 \qquad conv = 0$$
2) **Power scheduling update.** The scheduled power profiles of the individual appliances are iteratively updated:
WHILE $(conv = 0)$
   a) $conv = 1$
   b) $k = k+1$.
   c) $u(k) = u(k-1)$.
   d) **FOR** $j = 1:1:N$
      i) **FIND** $(\bar{t}^*, \underline{t}^*)$ such that:
$$(\bar{t}^*, \underline{t}^*) \in \underset{(\bar{t},\underline{t}) \in \mathscr{A}_j \times \mathscr{A}_j}{\arg\max} \gamma(u(k), j, \bar{t}, \underline{t})$$
      ii) **IF** $\gamma(u(k), j, \bar{t}^*, \underline{t}^*) > 0$
$$\begin{array}{cc} conv = 0 & \delta = \Delta(u(k), j, \bar{t}^*, \underline{t}^*) \\ u_{j,\bar{t}^*}(k) = u_{j,\bar{t}^*}(k) + \delta & u_{j,\underline{t}^*}(k) = u_{j,\underline{t}^*}(k) - \delta. \end{array}$$
   END FOR
   END WHILE
3) **Final results**. The Wardrop equilibrium solution is equal to the power scheduling at the last iteration:
$$u^* = u(k).$$

The power scheduling update described by (19) and (17) can be performed through Algorithm 1, graphically summarized by the flowchart in Fig. 1. The **Initialization phase** of the algorithm sets the power scheduling $u(0)$ of the whole population to some initial value u^0. In the **Power scheduling update** phase, each full execution of the **FOR** cycle in step 2.b) corresponds to the application of the mapping F in (19). In particular, each single iteration with index j is equivalent to the application of F_j in (17). First, the time instants $\bar{t}^*, \underline{t}^* \in \mathscr{A}_j$ which maximize γ are selected. Then, if the maximized γ is positive, the device j can reduce its energy cost by shifting the amount of power δ from $\underline{t}^*$ to $\bar{t}^*$. As established in Theorem 1, the algorithm converges to a Wardrop equilibrium. When $\gamma(u(k), j, \bar{t}_j, \underline{t}_j) \leq 0$ for all $j \in \mathscr{N}$ and $(\bar{t}_j, \underline{t}_j) \in \mathscr{A}_j \times \mathscr{A}_j$, the logical variable *conv* remains equal to 1 throughout the **FOR** cycle and the final scheduling $u^* = u(k)$, returned in the **Final results** phase, fulfills (13) in Proposition 3.

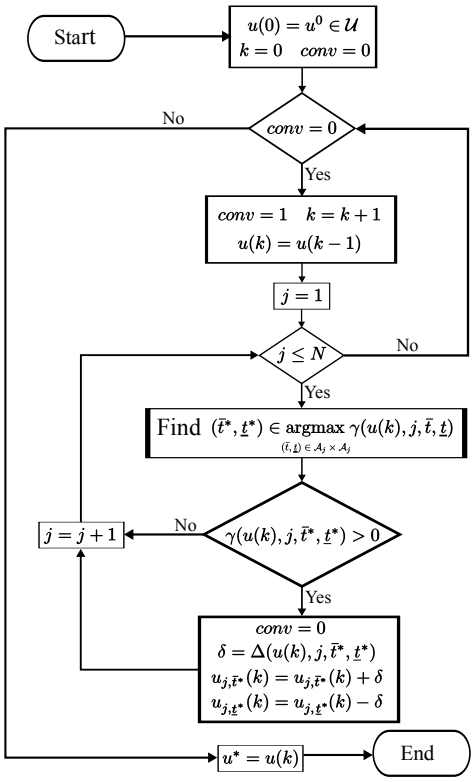

Fig. 1. Flowchart of Algorithm 1.

C. Implementation Scheme

Algorithm 1 constitutes a pseudo-code representation of the iterated application of the multi-valued mapping F in (19). It details the steps required to calculate the modified power schedule by each individual load and specifies the stopping criterion for the iterative updates. In the rest of this section, we present an implementation scheme for the application of this algorithm in a distributed way, considering iterated broadcast of prices and individual devices that autonomously modify their power schedule to reduce their costs. Relying on a bi-directional communication scheme between the system operator and the flexible loads, the operations associated to each step of the algorithm can be performed as follows:

1) **Initialization phase**: Each device j determines an initial feasible power consumption profile $u_j(0) = u_j^0 \in \mathscr{U}_j$. This can be obtained by broadcasting a certain price signal p to all the appliances and letting each device j schedule its power consumption $u_j(0) = u_j^0$ in order to minimize (9). The scheduled power profiles $u(0)$ are communicated to the central entity, which determines the resulting aggregate power demand $D(u(0))$ through (8).

2) **Power scheduling update**: Implementation of the **WHILE** cycle in step 2 can be performed as follows:

- The price signals $\bar{p}_{\mu_j}(D(u(k)))$ and $\underline{p}_{\mu_j}(D(u(k)))$, i.e. the locational marginal prices at bus $m=\mu_j$ associated to the current demand profile D are calculated according to (4) and broadcast to device j. This device can then independently determine the time instants $\bar{t}^*,\underline{t}^* \in \mathscr{A}_j$ of an advantageous power swap reducing its energy cost (as in step 2.b.iii of Algorithm 1).
- The device j applies (16) and independently calculates δ in step 2.b.iv of Algorithm 1, i.e. the maximum amount of power consumption that can be swapped in its power schedule from time $\underline{t}^*$ to $\bar{t}^*$.
- The device j communicates $\bar{t}^*$, $\underline{t}^*$ and δ to the central entity which in turn calculates the new demand profile $D(u(k+1))$ and the convergence flag *conv*.

3) **Final results**: When Algorithm 1 converges to a Wardrop equilibrium, as proven in Theorem 1, the **WHILE** cycle described above is concluded and the devices cannot further reduce their energy costs. Their final power profiles u_j^* will be equal to $u_j(k)$ at the last iteration k.

D. Methods for faster algorithm convergence

The coordination scheme in Algorithm 1 has been chosen for its simplicity and because it directly maps the multi-valued function F, introduced in (19) to analytically describe the scheduling update of the loads. Some alternative approaches that can ensure faster convergence are discussed below:

1) Multiple power swaps: Each load performs multiple simultaneous power swaps between distinct pairs of time instants that are characterized by advantageous price differentials. Within this framework, the convergence and optimality properties presented in Theorem 1 and 2 are preserved.

2) Best response strategy: Each load directly applies its cost-minimizing schedule in response to a price broadcast, with no impact of its previous power scheduling. This approach has exhibited fast convergence to equilibrium in simulation, but such result has not been formally proved.

3) One-shot strategy: With this method, discussed in detail in [15] for a simplified pricing structure, the flexible loads are coordinated through the broadcast of a single price signal (different in general for each load). These prices are calculated by the central coordinator, which receives the characteristics and task parameters of all the devices and internally emulates Algorithm 1 to calculate the final equilibrium solution. It should be mentioned that, in this case, one-shot convergence is obtained at the expenses of the loads' privacy.

V. Simulation Results

The performance of the proposed control scheme is assessed in simulation on the IEEE 24-bus system [31]. The generation cost $f_m(g)$ at each bus m is assumed to be a quadratic function of the power generation g, i.e. $f_m(g)=a_m g^2+b_m g$. A diagram with relevant quantities of the considered system is shown in Fig. 2 and all other parameters can be found in [31]. The inflexible active demand profiles $d_{m,t}$ are derived from historical data and are in general different for each bus. Their

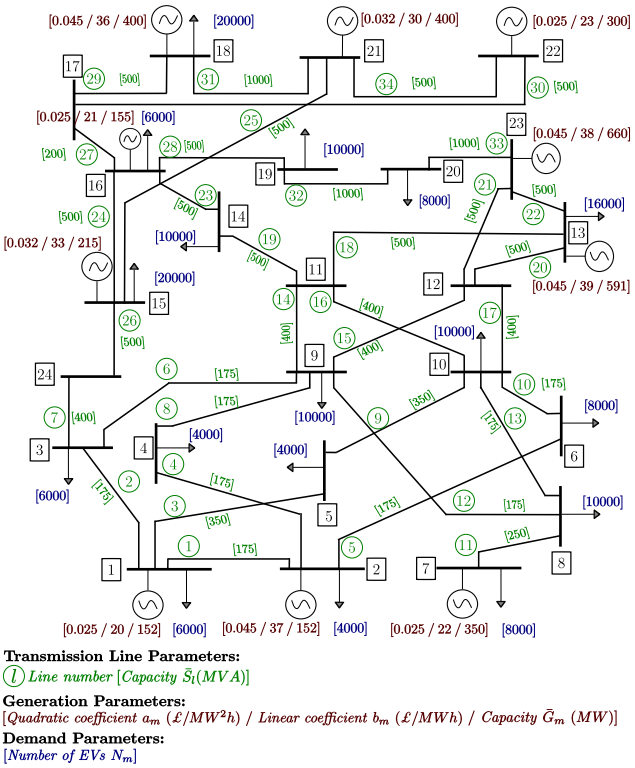

Fig. 2. Diagram of the IEEE 24-bus system.

values are shown in Fig. 3 (left - black dashed lines). It is assumed that all the inflexible loads operate at 0.95 lagging power factor and that, at each bus, the feasible range of voltage magnitudes is between 0.9 and 1.1 p.u.. Additionally, power losses are neglected. A future scenario with high penetration of electric vehicles is considered and $\mathscr{N}_m \subseteq \mathscr{N}$ represents the subset of N_m devices operating at bus m (chosen values of N_m are shown in Fig. 2). Each vehicle j is modelled as a load with unity power factor [32]. The required energy E_j of all devices $j \in \mathscr{N}_m$ is chosen according to a Gaussian distribution with mean x_m^E and standard deviation δ_m^E. In addition, it is assumed that all the vehicles at bus m have the same rated power P_m. For instance, the energy and power parameters for the EVs at bus 1 are selected as follows:

$$x_1^E = 30 \text{ kWh} \qquad \delta_1^E = 1\text{kWh} \qquad P_1 = 10\text{kW}.$$

The final time $T=24h$ and time discretization step $\Delta t = 0.25h$ are chosen for the considered time horizon. It is assumed that each vehicle j can operate in a continuous time interval $[t_j, t_j+d_j]$. The equivalent availability window $\mathscr{A}_j$ of the single device j can be expressed in discrete time as:

$$\mathscr{A}_j = \left\{ t \in \mathscr{T} : t_j \le t \cdot \Delta t \le t_j + d_j \right\}. \tag{24}$$

The values of t_j and d_j for all devices $j \in \mathscr{N}_m$ operating at bus m are also determined according to Gaussian distributions with mean values x_m^t and x_m^d and standard deviations δ_m^t and δ_m^d, respectively. For example, the availability parameters for the EVs at bus 1 are:

$$x_1^t = 21:30 \text{ h} \qquad \delta_1^t = 1.5 \text{ h} \qquad x_1^d = 10 \text{ h} \qquad \delta_1^d = 1.5 \text{ h}.$$

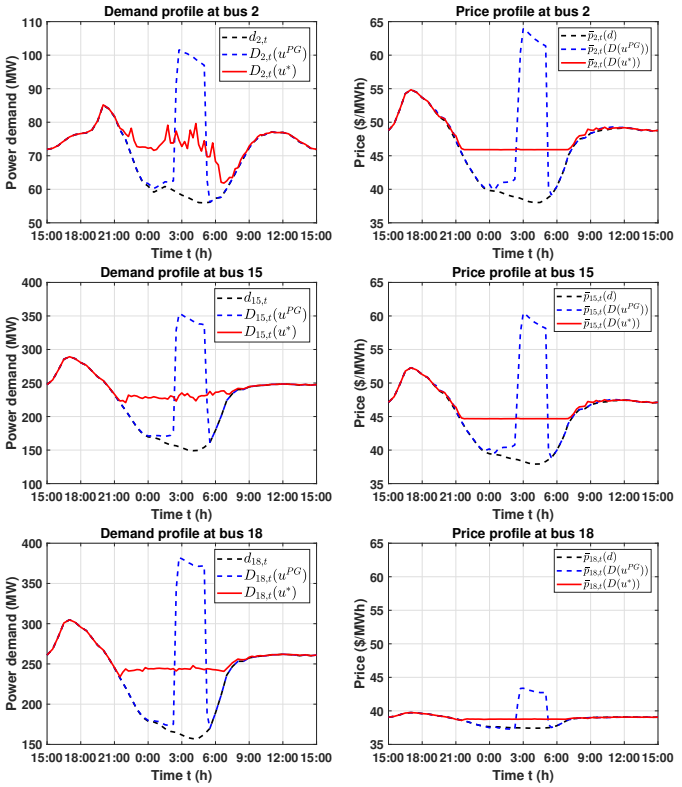

Fig. 3. Demand profiles (left) and electricity prices (right): no flexible demand (black dashed trace), with proposed scheduling (red trace) and **PG** scenario (blue dashed trace).

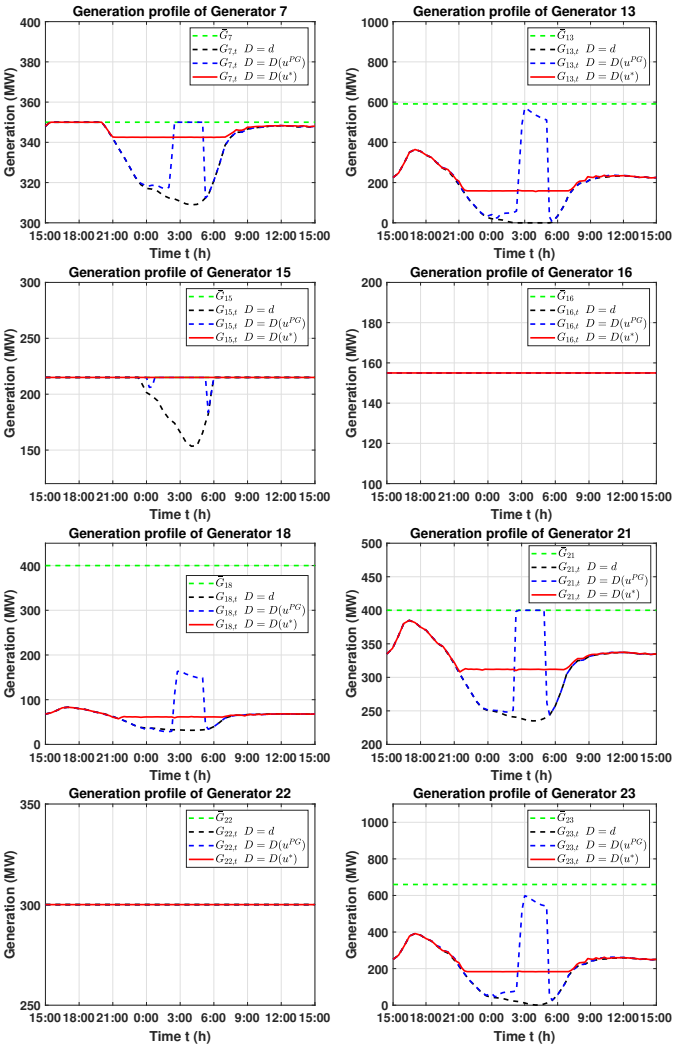

Fig. 4. Generation profiles: no flexible demand (black dashed trace), with proposed scheduling (red trace) and **PG** scenario (blue dashed trace).

It should be noted that the normal distributions used to generate the EVs parameters E_j, t_j and d_j are properly truncated and rescaled in order to ensure feasibility and well-posedness of the considered scheduling problem.

A. Algorithm Implementation

The coordination of the flexible devices has been performed with Algorithm 1. The initial condition $u(0) = u^0$ in Step 1) envisages constant power profiles for all loads. In the power update of Step 2), single devices have been sequentially selected at each iteration. A single power swap is performed as detailed in step 2.d) before moving on to the next device.

The final results of the proposed coordination scheme, denoted by the star superscript, have been compared with the scenario **PG** (price-greedy). In this latter case, a more naive approach is applied and each appliance $j \in \mathcal{N}_m$ determines its power consumption profile according to the price $\bar{p}_m(d)$, i.e. the electricity price when only inflexible demand d is considered. The total power consumption of the flexible appliances in this scenario is denoted as u^{PG}.

The demand and price profiles obtained with the two policies mentioned above are compared in Fig. 3. For length reasons, a limited number of relevant buses is considered. In the present case study, the two price signals $\bar{p}$ and $\underline{p}$ introduced in (4) coincide in all cases and therefore only the signal $\bar{p}$ is shown. The most relevant trend that we wish to emphasize is that the electricity price $\bar{p}_m(D(u^*))$ obtained with the proposed control strategy is consistently flatter than $\bar{p}_m(D(u^{PG}))$. All the electric vehicles schedule their charge between 22:00h and 7:00h, when the electricity price at their bus is constant and minimum. As expected, at equilibrium no device can exploit any price differential to reduce its energy cost and therefore has no unilateral interest in changing its final power consumption profile. Note that the same flattening trend, albeit on a lesser scale, appears in the demand profiles $D_m(u^*)$, which do not exhibit the significant rebound peaks of $D_m(u^{PG})$. The flattening of the demand profiles $D_m(u^*)$ in Fig. 3 is only partial since the iterative power update of the devices is based on differences in LMPs which, in general, do not exclusively depend on local demand but are also affected in non-trivial ways by the demand values at other buses.

The generation profiles obtained with the proposed control scheme and under the **PG** scenario are compared in Fig. 4. It can be seen that, differently from the significant variation experienced in the **PG** case, the presented coordination algorithm completely flattens generation at each bus during night-time.

Some relevant examples of apparent power flows (obtained with the proposed algorithm and in the **PG** case) are represented in Fig. 5. It can be seen that, in general, there

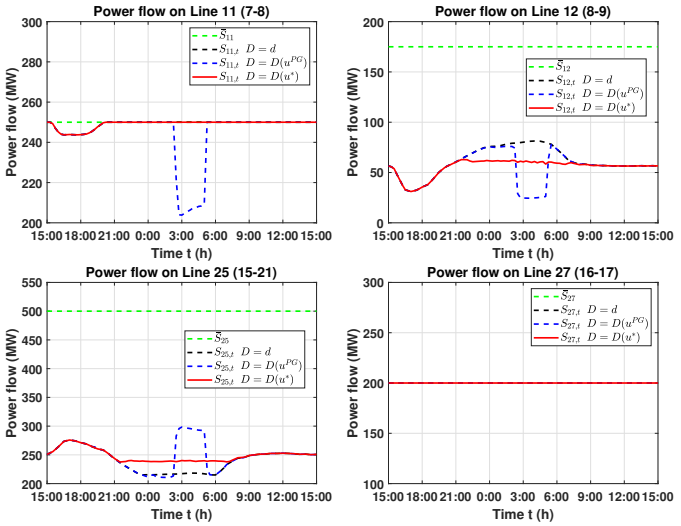

Fig. 5. Power flows: no flexible demand (black dashed trace), application of proposed scheduling (red trace) and **PG** scenario (blue dashed trace).

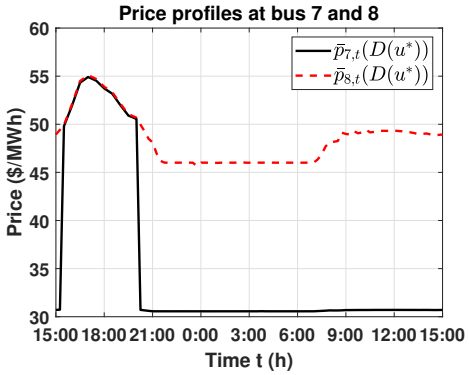

Fig. 6. The comparison of price profiles at buses 7 and 8 for $D = D(u^*)$.

are reduced variations over time when the final configuration with $D = D(u^*)$ is considered. Note also that line 27 always operates at its maximum capacity.

To assess the impact of generation capacity limits and lines congestion on the locational marginal prices, LMPs at buses 7 and 8 for $D = D(u^*)$ are plotted in Fig. 6. A few interesting trends can be underlined. As expected, the two prices $\bar{p}_{7,t}(D(u^*))$ and $\bar{p}_{8,t}(D(u^*))$ will be the same when there is no congestion on the line 11 connecting them (see top-left plot of Fig. 5). As soon as congestion appears on line 11, the prices become different: the LMP at bus 8 will vary continuously and its variations will be linked with the ones of other buses (i.e. buses 9 and 10), which are connected to bus 8 by lines 12 and 13 (not congested). Conversely, in this situation any additional unit of power at bus 7 can only be provided by generator 7 at its marginal generation cost, which leads to the negative price jump of $\bar{p}_{7,t}(D(u^*)$ (black trace).

B. Robustness with respect to uncertainties

The proposed control strategy operates under the assumption that the inflexible demand d is known without uncertainties and it does not explicitly account in its formulation for forecast errors on demand and generation. In order to

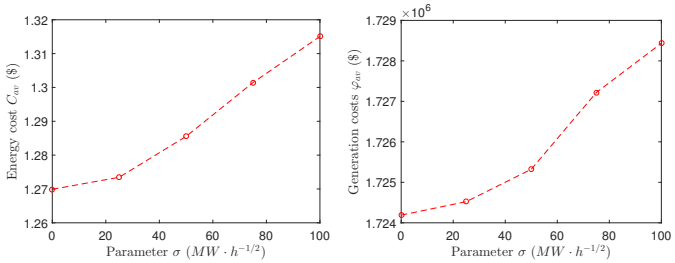

Fig. 7. Average energy cost C_{av} (left) and average generation costs φ_{av} (right) as functions of the parameter σ.

quantify the performance degradation when these elements are included in the case study, it is assumed that the coordination of the price-responsive loads is performed with an estimate $\tilde{d}$ of inflexible demand, which in general is different from the actual demand profile d. Denoting by $\tilde{d}_{m,t}$ the estimated inflexible demand at bus m and time t, we have:

$$\tilde{d}_{m,t} = d_{m,t} + \eta_{m,t} \tag{25}$$

where $\eta_{m,t}$ represents the forecast error on inflexible demand at bus m at time t. Assuming that renewable generation has zero marginal cost and it is always dispatched first, the quantity $\eta_{m,t}$ can equivalently represent a negative error forecast in renewable generation. The error forecast η_m is characterized as a random walk $\eta_{m,t+1} = \eta_{m,t} + \sigma_m e_t$, where e_t represents uncorrelated white noise with zero mean and unitary variance. With this formulation, consistently with basic models for wind error forecast, $\eta_{m,t}$ is a random variable with zero mean and standard deviation equal to $\sigma_m \cdot \sqrt{t}$. To account for error forecast correlation at the different buses due to geographical proximity, two independent noise signals e_t are considered for the South buses (e.g. buses 1-12) and for the North ones (buses 13-24). The value of σ_m at each node m is obtained as the rescaling of a unique parameter σ by the fraction of total demand at that node.

The coordination algorithm has been applied by considering the inflexible demand estimate $\tilde{d}$ rather than the actual profile d, denoting by $\tilde{u}^*$ the power scheduling of the appliances at the final equilibrium solution. In this case of imperfect information, the total generation costs will be equal to $\varphi(D(\tilde{u}^*))$ and the energy cost $\tilde{C}_j$ sustained by the single device j will correspond to:

$$\tilde{C}_j = \sum_{t=1}^{T} p_{\mu_j,t}(D(\tilde{u}^*)) \cdot \tilde{u}^*_{j,t} \cdot \Delta t$$

The optimal scheduling $\tilde{u}^*$ has been calculated over $L = 50$ realizations of the estimated inflexible demand profile $\tilde{d}$. The resulting cost C_{av} (average of $\tilde{C}_j$ over all devices and demand realizations) and the total generation costs φ_{av} (average of $\varphi(D(\tilde{u}^*))$ over all demand realizations) are plotted in Fig. 8 as a function of the standard deviation parameter σ.

As expected, for increasing values of σ (corresponding to higher forecast errors) the average energy cost C_{av} for the individual load and the average total generation costs φ_{av} increase. However, it can be seen that the performance degradation remains relatively small, even when large values of the standard deviation parameter σ are considered.

VI. Conclusions

This paper presents a novel distributed scheme for the coordination of large populations of flexible electric loads. A comprehensive modelling framework is proposed for demand response operating in multi-bus power systems, explicitly accounting for the congestion of transmission lines and the impact of flexible demand on the locational marginal prices at each bus. The main original contribution is a theoretical analysis that provides guarantees of convergence to a stable market outcome and global optimality, for any grid topology and penetration level of flexible demand. In addition, a double pricing structure and a novel concept of variational Wardrop equilibrium are proposed to characterize stable market configurations in the case of discontinuous price functions. Practical implementation of the presented control scheme is discussed and its performance is evaluated in simulation on the IEEE 24-bus system with high penetration of electric vehicles.

The analysis in this paper only considers the impact of price-responsive loads on the transmission infrastructure. Future work will expand the existing modelling framework to account for the effect of flexible demand on the distribution network. The approach proposed by [23] will initially be investigated, adding the contribution of flexible demand to the base load and adopting proper simulation tools to quantify the resulting load flows. A theoretical study will also be conducted, evaluating whether the presented results of convergence and optimality can be extended to a double-level network topology which accounts for transmission and distribution at the same time. Finally, the possibility of conducting a stochastic optimization which explicitly models and accounts for uncertainties on demand and generation will be explored.

References

[1] Electric Power Research Institute, "Environmental assessment of plug-in hybrid electric vehicles," California, USA, Tech. Rep., Jul. 2007.

[2] F. Rahimi and A. Ipakchi, "Demand response as a market resource under the smart grid paradigm," *IEEE Transactions on Smart Grid*, vol. 1, no. 1, pp. 82–88, 2010.

[3] S. Rahman and G. Shrestha, "An investigation into the impact of electric vehicle load on the electric utility distribution system," *IEEE Transactions on Power Delivery*, vol. 8, no. 2, pp. 591–597, 1993.

[4] K. Clement-Nyns, H. Edwin, and J. Driesen, "The impact of charging plug-in hybrid electric vehicles on a residential distribution grid," *IEEE Transactions on Power Systems*, vol. 25, no. 2, pp. 371–380, 2010.

[5] G. Strbac, "Demand side management: Benefits and challenges," *Energy policy*, vol. 36, no. 2, pp. 4419–4426, 2008.

[6] C. L. Su and D. Kirschen, "Quantifying the effect of demand response on electricity markets," *IEEE Transactions on Power Systems*, vol. 24, no. 3, pp. 1199–1207, 2009.

[7] Y. He, B. Venkatesh, and L. Guan, "Optimal scheduling for charging and discharging of electric vehicles," *IEEE Transactions on Smart Grid*, vol. 3, no. 3, pp. 1095–1105, 2012.

[8] E. Sortomme, M. M. Hindi, S. J. MacPherson, and S. S. Venkata, "Coordinated charging of plug-in hybrid electric vehicles to minimize distribution system losses," *IEEE Transactions on Smart Grid*, vol. 2, no. 1, pp. 198–205, 2011.

[9] Y. Zhang, N. Gatsis, and G. B. Georgios, "Robust energy management for microgrids with high-penetration renewables," *IEEE Transactions on Sustainable Energy*, vol. 4, no. 4, pp. 944–953, 2013.

[10] Z. Fan, "A distributed demand response algorithm and its application to phev charging in smart grids," *IEEE Transactions on Smart Grid*, vol. 3, no. 3, pp. 1280–1290, 2012.

[11] L. Gan, U. Topcu, and S. H. Low, "Stochastic distributed protocol for electric vehicle charging with discrete charging rate," in *Power and Energy Society General Meeting, 2012 IEEE*, 2012, pp. 1–8.

[12] A. Mohsenian-Rad, V. Wong, J. Jatskevich, R. Schober, and A. Leon-Garcia, "Autonomous demand-side management based on game-theoretic energy consumption scheduling for the future smart grid," *IEEE Transactions on Smart Grid*, vol. 1, no. 3, pp. 320–331, 2010.

[13] L. Gan, U. Topcu, and S. H. Low, "Optimal decentralized protocol for electric vehicle charging," *IEEE Transactions on Power Systems*, vol. 28, no. 2, pp. 940–951, 2013.

[14] Z. Ma, D. Callaway, and I. Hiskens, "Decentralized charging control of large populations of plug-in electric vehicles," *IEEE Transactions on Control Systems Technology*, vol. 21, no. 1, pp. 67–78, 2013.

[15] A. De Paola, D. Angeli, and G. Strbac, "Price-based schemes for distributed coordination of flexible demand in the electricity market," *IEEE Transactions on Smart Grid*, vol. 8, no. 6, pp. 3104–3116, 2017.

[16] B. G. Kim, S. Ren, M. van der Schaar, and J. W. Lee, "Bidirectional energy trading and residential load scheduling with electric vehicles in the smart grid," *IEEE Journal on Selected Areas in Communications*, vol. 31, no. 7, pp. 1219–1234, 2013.

[17] H. Chen, Y. Li, R. Louie, and B. Vucetic, "Autonomous demand side management based on energy consumption scheduling and instantaneous load billing: An aggregative game approach," *IEEE Transactions on Smart Grid*, vol. 5, no. 4, pp. 1744–1754, 2014.

[18] Z. Ma, S. Zou, X. S. L. Ran, and I. Hiskens, "Efficient decentralized coordination of large-scale plug-in electric vehicle charging," *Automatica*, vol. 69, pp. 35–47, 2016.

[19] M. González Vayá, T. Krause, R. A. Waraichand, and G. Andersson, "Locational marginal pricing based impact assessment of plug-in hybrid electric vehicles on transmission networks," in *CIGRE International Symposium*, Bologna, Italy, 2011.

[20] L. Wang, "Potential impacts of plug-in hybrid electric vehicles on locational marginal prices," in *IEEE Energy 2030 Conf.*, Atlanta, 2008.

[21] L. Wu, "Impact of price-based demand response on market clearing and locational marginal prices," *IET Generation, Transmission & Distribution*, vol. 7, no. 10, pp. 1087–1095, 2013.

[22] Y. Wang, L. Wu, and S. Wang, "A fully-decentralized consensus-based admm approach for dc-opf with demand response," *IEEE Transactions on Smart Grid*, vol. 8, no. 6, pp. 2637–2647, 2017.

[23] M. González Vayá, M. D. Galus, R. A. Waraich, and G. Andersson, "On the interdependence of intelligent charging approaches for plug-in electric vehicles in transmission and distribution networks," in *Proc. IEEE PES Innovative Smart Grid Technologies Europe*, Berlin, 2012.

[24] C. Zhao, J. Wang, J. Watson, and Y. Guan, "Multi-stage robust unit commitment considering wind and demand response uncertainties," *IEEE Trans. on Power Systems*, vol. 28, no. 3, pp. 2708–2717, 2013.

[25] A. De Paola, D. Angeli, and G. Strbac, "Convergence and optimality of a new iterative price-based scheme for distributed coordination of flexible loads in the electricity market," in *Proceedings of the IEEE Conference on Decision and Control*, Melbourne, 2017, pp. 1386–1393.

[26] Z. Yang, H. Zhong, A. Bose, T. Zheng, Q. Xia, and C. Kang, "Linearized OPF model with reactive power and voltage magnitude: a pathway to improve the mw-only DC OPF," *IEEE Transactions on Power Systems*, vol. 33, no. 2, pp. 1734–1745, 2018.

[27] T. Akbari and M. T. Bina, "Linear approximated formulation of ac optimal power flow using binary discretisation," *IET Generation, Transmission & Distribution,*, vol. 10, no. 5, pp. 1117–1123, 2016.

[28] L. C. Evans and R. F. Gariepy, *Measure theory and fine properties of functions*. Boca Raton, FL: CRC, 1992.

[29] S. Grammatico, "Dynamic control of agents playing aggregative games with coupling constraints," *IEEE Transactions on Automatic Control*, vol. 62, no. 9, pp. 4537–4548, 2017.

[30] B. Gentile, F. Parise, D. Paccagnan, M. Kamgarpour, and J. Lygeros, "Nash and wardrop equilibria in aggregative games with coupling constraints," *arXiv preprint arXiv: 1702.08789*, 2017.

[31] Probability Methods Subcommittee, "IEEE reliability test system," *IEEE Trans. on Power App. Syst.*, vol. PAS-98, no. 6, pp. 2047–2054, 1979.

[32] P. Richardson, D. Flynn, and A. Keane, "Optimal charging of electric vehicles in low-voltage distribution systems," *IEEE Transactions on Power Systems*, vol. 27, no. 1, pp. 268–279, 2012.

[33] R. K. Sundaram, *A first course in optimization theory*. New York: Cambridge Univ. Press, 1996.

[34] F. H. Clarke, *Optimization and Nonsmooth Analysis*. NY: Wiley, 1983.

[35] R. Goebel, R. G. Sanfelice, and A. R. Teel, *Hybrid Dynamical Systems*. Princeton University Press, 2012.

[36] A. L. Dontchev and R. T. Rockafellar, *Implicit Functions and Solution Mappings*. Springer, 2009.

[37] C. D. Aliprantis and K. C. Border, *Infinite Dimensional Analysis*. Springer, 2007.

APPENDIX A
PROOF OF PROPOSITION 1

Two key points are preliminarily shown. Firstly, the objective function in the right-hand side of (1) is strictly convex given the strict convexity of each f_m. Secondly, let $\mathscr{G}(D)$ denote the set of feasible solution vectors – including active and reactive power generation (G, GQ), voltage angle and squared magnitude (θ, v^2) – that fulfill (2) for a certain $D \in \mathbb{R}^{MT}$. The graph of $\mathscr{G}$ is convex. This property follows from the linearity and convexity of the constraints in (2). As a result, the strict convexity of $\varphi(D)$ with respect to D follows from the maximum theorem under convexity [33].

APPENDIX B
PROOF OF PROPOSITION 2

For simplicity, we consider the simplified case in which the minimized generation cost $\varphi(D)$ in (1) is always differentiable. As a result, prices at bus m at time t are unique and equal to:

$$\bar{p}_{m,t}(D) = \underline{p}_{m,t}(D) = p_{m,t}(D) = \frac{\partial \varphi(D)}{\partial D_{m,t}}. \tag{26}$$

From Proposition 1, we have that $\varphi(D)$ is a strictly convex function and therefore its Hessian matrix H is positive definite, with $H \succ 0$. From basic properties of positive definite matrices, the following holds for each diagonal element of H:

$$\frac{\partial^2 \varphi(D)}{\partial D_{m,t}^2} > 0 \quad \forall t, m. \tag{27}$$

To verify the proposition statement, it is sufficient to check the positivity of the following partial derivative:

$$\frac{\partial p_{m,t}(D)}{\partial D_{m,t}} = \frac{\partial}{\partial D_{m,t}} \left(\frac{\partial \varphi(D)}{\partial D_{m,t}} \right) = \frac{\partial^2 \varphi(D)}{\partial D_{m,t}^2} > 0 \quad \forall t, m. \tag{28}$$

APPENDIX C
PROOF OF PROPOSITION 3

Each feasible power schedule u_j for agent j can be expressed as the sum of the strategy u_j^* at the candidate equilibrium solution plus a finite number Q of elementary variations:

$$u_j = u_j^* + \sum_{q=1}^{Q} \delta_q \tag{29}$$

where each term $\delta_q : \mathscr{T} \to \mathbb{R}$, for some $\Delta_q > 0$ and $(\bar{t}_q, \underline{t}_q) \in \mathscr{A}_j \times \mathscr{A}_j$ has the following expression:

$$\delta_{q,t} = \Delta_q \cdot \mathbb{1}_{\{\bar{t}_q\}}(t) - \Delta_q \cdot \mathbb{1}_{\{\underline{t}_q\}}(t). \tag{30}$$

The above expressions can represent all the elements $u_j \in \mathscr{U}_j$, since these are characterized by the same fixed sum. In addition, one can assume without loss of generality that each δ_q corresponds to a feasible power swap of Δ_q between the time instants $\bar{t}_q$ and $\underline{t}_q$. As a result, it must hold:

$$0 < \Delta_q \leq \min\left(\left\{ P_j - u_{j,\bar{t}_q}^*, u_{j,\underline{t}_q}^* \right\} \right) \tag{31}$$

If one substitutes (29) in (10), the cost variation ΔC_j can be written as:

$$\Delta C_j = \sum_q \left[\bar{p}_{\mu_j,\bar{t}_q}^*(D(u^*)) - \underline{p}_{\mu_j,\underline{t}_q}^*(D(u^*)) \right] \Delta_q \Delta t \tag{32}$$

Suppose that $\Delta C_j < 0$ for some $u_j \in \mathscr{U}_j$. From (31) and (32) there should exist $\hat{q} \leq Q$ such that the following holds:

$$\bar{p}_{\mu_j,\bar{t}_{\hat{q}}}^*(D(u^*)) \leq \underline{p}_{\mu_j,\underline{t}_{\hat{q}}}^*(D(u^*)) \quad u_{j,\bar{t}_{\hat{q}}}^* < P_j \quad u_{j,\underline{t}_{\hat{q}}}^* > 0. \tag{33}$$

This would imply $\gamma(u^*, j, \bar{t}_{\hat{q}}, \underline{t}_{\hat{q}}) > 0$, thus proving the proposition statement by contradiction.

APPENDIX D
PROOF OF PROPOSITION 4

Proof of (21a): An equivalent condition is verified:

$$\varphi(D(u^+)) \leq \varphi(D(u)) \qquad \forall u^+ \in F(u),\ \forall u \in \mathscr{U}. \tag{34}$$

From (19), F is the composition of N elementary mappings F_j, defined in (17). Therefore, a slightly stronger condition can be proven by means of inequalities on each F_j:

$$\varphi(D(y)) \leq \varphi(D(u)) \qquad \forall y \in F_j(u), \forall j \in \mathscr{N},\ \forall u \in \mathscr{U}. \tag{35}$$

Note that (35) holds if, for all $s_j(u) = (\bar{t}_j, \underline{t}_j) \in S_j(u)$, we have:

$$\varphi\left(D\left(f^{(s_j(u))} \right) \right) < \varphi\left(D(u) \right) \qquad \text{if } \gamma(u, j, \bar{t}_j, \underline{t}_j) > 0 \tag{36a}$$

$$\varphi\left(D\left(f^{(s_j(u))} \right) \right) = \varphi\left(D(u) \right) \qquad \text{if } \gamma(u, j, \bar{t}_j, \underline{t}_j) \leq 0 \tag{36b}$$

For the case of (36a) with $\gamma(u, j, \bar{t}_j, \underline{t}_j) > 0$, since by definition $u_{j,\bar{t}_j} \leq P_j$ and $u_{j,\underline{t}_j} \geq 0$, as a result of (12) it holds:

$$\left(\underline{p}_{\mu_j,\underline{t}}(D(u)) - \bar{p}_{\mu_j,\bar{t}}(D(u)) \right) > 0 \quad u_{j,\bar{t}_j} < P_j \quad u_{j,\underline{t}_j} > 0. \tag{37}$$

For the function ε in (5), given the monotonicity of $\bar{p}$ and $\underline{p}$ established in Proposition 2, we have:

$$\varepsilon\left(D(u), \mu_j, \bar{t}_j, \underline{t}_j \right) > 0 \tag{38}$$

which implies positivity of Δ in (16), as a result of (37):

$$\Delta(u, \mu_j, \bar{t}_j, \underline{t}_j) = \bar{\Delta} > 0. \tag{39}$$

Recalling expressions (8) and (18), and applying the mean value theorem for non-smooth functions [34], the left-hand side in (36a) can be rewritten as follows:

$$\begin{aligned} \varphi\left(D\left(f^{(s_j(u))} \right) \right) &= \varphi\left(D\left(u + \bar{\Delta}\left(\hat{\mathbf{e}}_{j,\bar{t}_j} - \hat{\mathbf{e}}_{j,\underline{t}_j} \right) \right) \right) \\ &= \varphi\left(D(u) + \bar{\Delta}\left(\hat{\mathbf{e}}_{\mu_j,\bar{t}_j} - \hat{\mathbf{e}}_{\mu_j,\underline{t}_j} \right) \right) \\ &= \varphi(D(u)) + \left\langle \partial\varphi(\tilde{D}), \bar{\Delta}\left(\hat{\mathbf{e}}_{\mu_j,\bar{t}_j} - \hat{\mathbf{e}}_{\mu_j,\underline{t}_j} \right) \right\rangle \end{aligned} \tag{40}$$

where $\tilde{D}$ is some convex combination of $D(u)$ and $D\left(f^{(s_j(u))} \right)$ and $\partial\varphi$ denotes the generalized gradient of φ. From Proposition 1, this corresponds to the subdifferential of φ. The above equation can now be rewritten as:

$$\varphi\left(D\left(f^{(s_j(u))} \right) \right) = \varphi\left(D(u) \right) + \bar{\Delta}\left(\bar{p}^* - \underline{p}^* \right) \tag{41}$$

with $\bar{p}^* \in \frac{\partial\varphi(\tilde{D})}{\partial D_{\mu_j,\bar{t}_j}}$ and $\underline{p}^* \in \frac{\partial\varphi(\tilde{D})}{\partial D_{\mu_j,\underline{t}_j}}$. Condition (36a) is therefore verified by the positivity of $\bar{\Delta}$ in (39) and the following:

$$\begin{aligned} \bar{p}^* &\overset{(a)}{\leq} \bar{\varphi}'_{\mu_j,\bar{t}_j}(\tilde{D}) \overset{(b)}{<} \bar{p}_{\mu_j,\bar{t}_j}\left(D\left(f^{(s_j(u))} \right) \right) \\ &\overset{(c)}{\leq} \underline{p}_{\mu_j,\underline{t}_j}\left(D\left(f^{(s_j(u))} \right) \right) \overset{(d)}{<} \underline{\varphi}'_{\mu_j,\underline{t}_j}(\tilde{D}) \overset{(e)}{\leq} \underline{p}^*. \end{aligned} \tag{42}$$

The inequalities (a) and (e) follow from (3) and (4), (b) and (d) are a result of Proposition 2 and (c) holds by construction of $\varepsilon(D(u),\mu_j,\bar{t}_j,\underline{t}_j)$ as expressed in (5) in Definition 1. We can conclude that (36a) holds as a result of (41) and (42). Similar arguments can be used to also verify (36b), thus proving (21a).

Proof of (21b): Since φ is nonincreasing when any F_j is applied, (36b) must hold for all $j \in \mathscr{N}$ when $u = \psi(k)$ and $\varphi(\psi(k+1)) = \varphi(\psi(k))$. As previously proved, this implies $\Delta(u,\mu_j,\bar{t}_j,\underline{t}_j) = 0$ for all j and therefore $\psi(k+1) = \psi(k)$.

Proof of (21c): This property straightly follows from (21a) and the boundedness of φ.

Appendix E
Proof of Theorem 1

Consider the omega-limit set $\Omega(\psi)$ associated to the solution $\psi \in \Psi$ and defined as follows:

$$\Omega(\psi) := \left\{ u_\infty : \exists \{k_n\}_{n\in\mathbb{N}},\ \lim_{n\to\infty} k_n = \infty,\ \lim_{n\to\infty} \psi(k_n) = u_\infty \right\}. \tag{43}$$

The theorem is verified if the following holds for all $\psi \in \Psi$:

$$\lim_{k\to\infty} |\psi(k)|_{\Omega(\psi)} = 0 \tag{44a}$$

$$\Omega(\psi) \subseteq \Omega^*. \tag{44b}$$

Condition (44a): this result holds if the mapping F is upper-semicontinuous [35, Chapter 6.3.3]. Since F takes non-empty compact values, the upper-semicontinuity of the mapping is guaranteed by F having a closed graph $\mathscr{G}$ [36, Chapter 3B]. Accounting for the compactness of $\mathscr{U}$, it is sufficient to show that the graph $\mathscr{G}_j$ of the individual mappings F_j in (19) is closed [37]. The graph $\mathscr{G}_j$ can be expressed as:

$$\begin{aligned}\mathscr{G}_j &= \left\{ (u, f^{(s_j)}(u)) : u \in \mathscr{U},\ f^{(s_j)}(u) \in F_j(u) \right\} \\ &= \bigcup_{s_j \in \mathscr{A}_j \times \mathscr{A}_j} \mathscr{G}^{(s_j)} = \bigcup_{s_j \in \mathscr{A}_j \times \mathscr{A}_j} \left\{ (u, f^{(s_j)}(u)) : u \in U^{(s_j)} \right\}.\end{aligned} \tag{45}$$

where $U^{(s_j)} \subseteq \mathscr{U}$ has the following expression:

$$\begin{aligned}U^{(s_j)} &= \{\ u \in \mathscr{U} : s_j = (\bar{t}_j,\underline{t}_j) \in S_j(u)\ \} \\ &= \{\ u \in \mathscr{U} : s_j = (\bar{t}_j,\underline{t}_j), \\ &\qquad \gamma(u,j,\bar{t}_j,\underline{t}_j) \geq \gamma(u,j,\bar{t},\underline{t})\ \forall (\bar{t},\underline{t}) \in \mathscr{A}_j \times \mathscr{A}_j \}.\end{aligned} \tag{46}$$

One can verify that $\mathscr{G}^{(s_j)}$ is closed since the state-space subset $U^{(s_j)}$ is closed (defined by a set of non-strict inequalities) and each component $f^{(s_j)}_{i,t}(u)$ of $f^{(s_j)}(u)$ in (17) is continuous with respect to u. This means that also $\mathscr{G}_j$ is closed (union of a finite number of closed sets), thus proving the closedness of $\mathscr{G}$, the upper semi-continuity of F and condition (44a).

Condition (44b): To verify that each point in $\Omega(\psi)$ also belongs to the set of variational Wardrop equilibria Ω^*, it is preliminarily shown that, as a result of (21c) and continuity of φ and D, the following holds for all $u_\infty \in \Omega(\psi)$:

$$\begin{aligned}\varphi(D(u_\infty)) &= \varphi\left(D\left(\lim_{n\to\infty} \psi(k_n)\right)\right) = \lim_{n\to\infty} \varphi(D(\psi(k_n))) \\ &= \lim_{k\to\infty} \varphi(D(\psi(k))) = \varphi_\infty.\end{aligned} \tag{47}$$

Moreover, as a result of the outer-semicontinuity of the mapping F, weak-forward invariance of $\Omega(\psi)$ is also guaranteed [35, Chapter 6.3.3]:

$$F(u_\infty) \cap \Omega(\psi) \neq \varnothing \qquad \forall u_\infty \in \Omega(\psi). \tag{48}$$

As (47) establishes that all points $u_\infty \in \Omega(\psi)$ have equal generation costs φ_∞ and φ is non decreasing along all trajectories ψ, there must exist $s_1 = (\bar{t}_1,\underline{t}_1) \in S_1(u_\infty)$ such that:

$$\varphi\left(D\left(f^{(s_1)}(u_\infty)\right)\right) = \varphi(D(u_\infty)) \qquad \gamma(u_\infty,1,\bar{t}_1,\underline{t}_1) \leq 0. \tag{49}$$

If this were not the case, from (19) and (21a), we would have:

$$\varphi(D(u^+)) < \varphi(D(u_\infty)) \qquad \forall u^+ \in F(u_\infty)$$

which contradicts (48) if one considers (47). As γ is maximized by all $s \in S_1(u_\infty)$ from (15), we have:

$$\gamma(u_\infty,1,\bar{t},\underline{t}) \leq 0 \quad \forall s = (\bar{t},\underline{t}) \in S_1(u_\infty). \tag{50a}$$

$$\Delta(u_\infty,1,\bar{t},\underline{t}) = 0 \quad \forall s = (\bar{t},\underline{t}) \in S_1(u_\infty) \tag{50b}$$

where (50b) also implies $F_1(u_\infty) = \{u_\infty\}$. Recursive application of the same arguments for $j = 2,\dots,N$ yields:

$$\gamma(u_\infty,j,\bar{t},\underline{t}) \leq 0 \quad \forall s_j = (\bar{t},\underline{t}) \in S_j(u_\infty), \forall j \in \mathscr{N}. \tag{51}$$

The proof of (44b) is concluded by noting that, from (15), conditions (51) and (13) in Proposition 3 when $u^* = u_\infty$.

Appendix F
Proof of Theorem 2

Given the differentiability of $\varphi(D(u^*))$, the following gradient vector can be derived from (3):

$$\nabla_m \varphi(D) = \left[\frac{\partial \varphi(D)}{\partial D_{m,1}}, \dots, \frac{\partial \varphi(D)}{\partial D_{m,T}} \right] = \left[\varphi'_{m,1}(D), \dots, \varphi'_{m,T}(D) \right]. \tag{52}$$

From the strict convexity of $\varphi(D)$ in Proposition 1, it is sufficient to prove the following local condition for any $u \in \mathscr{U}$:

$$\begin{aligned}&\langle \nabla_m \varphi(D(u^*)), D_m(u) - D_m(u^*) \rangle \\ &\quad = \sum_{t=1}^{T} \varphi'_{m,t}(D(u^*)) \cdot [D_{m,t}(u) - D_{m,t}(u^*)] \\ &\quad = \sum_{t=1}^{T} \varphi'_{m,t}(D(u^*)) \left[\sum_{j:\mu_j = m} u_{j,t} - u^*_{j,t} \right] \geq 0\end{aligned} \qquad \forall m \in \mathscr{M}. \tag{53}$$

We recall that any $u \in \mathscr{U}$ can be characterized as the sum of u^* and a finite number Q of power swaps δ_q, as presented in equations (29)-(30) in the proof of Proposition 3. Therefore, condition (53) holds if the following is verified for all $j \in \mathscr{N}$:

$$\begin{aligned}\sum_{t=1}^{T} \varphi'_{\mu_j,t}(D(u^*)) \left[u_{j,t} - u^*_{j,t} \right] &= \sum_{t=1}^{T} \varphi'_{\mu_j,t}(D(u^*)) \left[\sum_{q=1}^{Q} \delta_{q,t} \right] \\ &= \sum_{q=1}^{Q} \Delta_q \left[\varphi'_{\mu_j,\bar{t}_q}(D(u^*)) - \varphi'_{\mu_j,\underline{t}_q}(D(u^*)) \right] \\ &= \sum_{q=1}^{Q} \Delta_q \left[\bar{p}_{\mu_j,\bar{t}_q}(D(u^*)) - \underline{p}_{\mu_j,\underline{t}_q}(D(u^*)) \right] \geq 0.\end{aligned} \tag{54}$$

Consider now the equilibrium condition (13) in Proposition 3. From expression (12) of γ and recalling (31) from the feasibility of δ_q, one can conclude that $\underline{p}_{\mu_j,\underline{t}_q}(D(u^*)) \leq \bar{p}_{\mu_j,\bar{t}_q}(D(u^*))$ at the equilibrium $u^* \in \Omega^*$, thus proving (54) and the theorem.

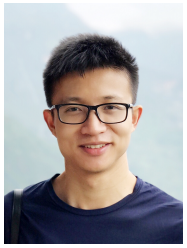

Xuan Gong received the B.Eng. degree in electrical engineering and automation from Huazhong University of Science and Technology, Wuhan, China in 2015, the M.Sc. degree in Future Power Networks from Imperial College London, London, U.K. in 2016, where he is currently pursuing a Ph.D. degree in electrical engineering. His current research interests include game theory and the design of novel distributed control strategies for the smart grid.

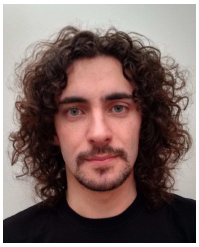

Antonio De Paola (M'15) received the M.Sc. degree in control engineering from the University of Rome Tor Vergata, Rome, Italy, in 2011, and the Ph.D. degree in electrical and electronic engineering from Imperial College London, London, U.K., in 2015. In 2017 he was awarded an Early Career Fellowship from the Leverhulme Trust and he is currently a Lecturer at the University of Bath. His main research interests include optimal control and game theory, with a specific focus on the design of novel control and market solutions for the deployment of a sustainable and decarbonized electricity grid.

David Angeli (F'15) was born in Siena, Italy, in 1971. He received the B.S. degree in Computer Science Engineering and the Ph.D. in Control Theory from University of Florence, Italy, in 1996 and 2000, respectively. Since 2000 he was an Assistant and Associate Professor (2005) with the Department of Systems and Computer Science, University of Florence. In 2007 he was a visiting Professor with I.N.R.I.A de Rocquencourt, Paris, France, and since 2008, he joined as a Senior Lecturer the Department of Electrical and Electronic Engineering of Imperial College London, where he is currently a Reader in Nonlinear Control and the Director of the MSc in Control Systems. He is a Fellow of IEEE and of IET. He has served as an Associate Editor for IEEE Transactions in Automatic Control and Automatica. Overall he authored more than 100 journal papers in the areas of Stability of nonlinear systems, Control of constrained systems (MPC), Chemical Reaction Networks theory and Smart Grids.

Goran Strbac (M'95) is a Professor of energy systems at Imperial College London, London. His current research is focused on modelling and optimization of economic and security performance of energy system operation and investment, including analysis of future energy markets to support cost effective transition to smart low carbon energy future.